

# Eclipsing binaries in extrasolar planet transit surveys: the case of SuperWASP

B. Willems<sup>1\*</sup>, U. Kolb<sup>2,\*</sup> and S. Justham<sup>2,3,\*</sup>

<sup>1</sup>*Northwestern University, Department of Physics and Astronomy, 2145 Sheridan Road, Evanston, IL 60208, USA*

<sup>2</sup>*Department of Physics and Astronomy, The Open University, Walton Hall, Milton Keynes, MK7 6AA, UK*

<sup>3</sup>*Department of Astrophysics, Oxford University, Oxford OX1 3RH, UK*

Accepted ... Received ...; in original form ...

## ABSTRACT

Extrasolar planet transit surveys will also detect eclipsing binaries. Using a comprehensive binary population synthesis scheme, we investigate the statistical properties of a sample of eclipsing binaries that is detectable by an idealised extrasolar planet transit survey with specifications broadly similar to those of the SuperWASP (Wide Angle Search for Planets) project.

In this idealised survey the total number of detectable single stars in the Galactic disc is of the order of  $10^6 - 10^7$ , while, for a flat initial mass ratio distribution, the total number of detectable eclipsing binaries is of the order of  $10^4 - 10^5$ . The majority of the population of detectable single stars is made up of main-sequence stars ( $\approx 60\%$ ), horizontal-branch stars ( $\approx 20\%$ ), and giant-branch stars ( $\approx 10\%$ ). The largest contributions to the population of detectable eclipsing binaries stem from detached double main-sequence star binaries ( $\approx 60\%$ ), detached giant-branch main-sequence star binaries ( $\approx 20\%$ ), and detached horizontal-branch main-sequence star binaries ( $\approx 10\%$ ). White dwarf main-sequence star binaries make up approximately 0.3% of the sample.

The ratio of the number of eclipsing binaries to the number of single stars detectable by the idealised SuperWASP survey varies by less than a factor of 2.5 across the sky, and decreases with increasing Galactic latitude. It is found to be largest in the direction of the Galactic longitude  $l = -7.5^\circ$  and the Galactic latitude  $b = -22.5^\circ$ .

We also show that the fractions of systems in different subgroups of eclipsing binaries are sensitive to the adopted initial mass ratio or initial secondary mass distribution, which is one of the poorest constrained input parameters in present-day binary population synthesis calculations. This suggests that once statistically meaningful results from transit surveys are available, they will be able to significantly improve the predictive power of population synthesis studies of interacting binaries and related objects.

**Key words:** surveys – binaries: eclipsing – stars: evolution – stars: statistics – Galaxy: stellar content

## 1 INTRODUCTION

An ever increasing number of extrasolar planets is being discovered (to date the number stands at more than 160), mostly through the detection of the reflex motion of their parent star around the planetary system’s centre of mass. Planets with suitably oriented orbits in space may also reveal their presence when they transit the disc of their parent star and the transit is accompanied by a measurable decrease in the observed stellar flux. When combined with high-precision radial-velocity measurements, the transits yield a wealth of information on the planet, such as its mass, radius, and mean density.

The first successful planetary transit detections were made independently by Charbonneau et al. (2000) and Henry et al. (2000), who observed a clear drop in the lightcurve of the star HD 209458 at times consistent with the ephemeris of its already known planetary-mass companion. Since then, the search for transits has rapidly evolved into a fully-fledged and widely used technique to hunt for extrasolar planets.

In anticipation of upcoming space-based exoplanet transit surveys such as COROT (scheduled to launch in 2006) and Kepler (scheduled to launch in 2007), ground-based surveys can pave the way towards obtaining a statistically significant sample of planets in a relatively short amount of time. Such a sample will be of great importance in improving our understanding of the formation and evolution of extrasolar planets as well as for detecting possible correlations between the presence of planets and the properties of their

\* E-mail: b-willems@northwestern.edu, u.c.kolb@open.ac.uk, sjustham@astro.ox.ac.uk

host stars. For an overview of some existing exoplanet transit surveys, we refer to the reviews by Horne (2002, 2003) and Charbonneau (2003). Despite the multitude of exoplanet transit surveys, so far only six confirmed planets have been discovered by direct observations of transits: five by the Optical Gravitational Lensing Experiment (OGLE) (Konacki et al. 2003; Konacki et al. 2004; Bouchy et al. 2004; Pont et al. 2004; Konacki et al. 2005), and one by the Trans-Atlantic Exoplanet Survey (TrES) network (Alonso et al. 2004).

Besides planetary transit detections, wide-field photometric transit searches will also yield a wealth of photometric data on all kinds of new and existing variable stars, including eclipsing binaries. Brown (2003) estimated the rate of false planetary detections due to eclipsing binaries with main-sequence and giant-type component stars to be almost an order of magnitude larger than the rate of true planetary detections. Examples of astrophysical false positives in wide-field transit searches are grazing incidence eclipses and the blending of the light of an eclipsing binary with the light of a third star (see Charbonneau et al. 2003 for details).

Our aim in this exploratory paper is to perform a binary population synthesis study to predict the statistical properties and the Galactic distribution of eclipsing binaries detectable by an extrasolar planet transit survey, and to investigate their dependency on the initial mass ratio distribution of the component stars. Specifically, we study the detectable sample for an idealised survey that is broadly representative of the ground-based SuperWASP Wide Angle Search for Planets (Kane et al. 2003, 2004; Street et al. 2003, Christian et al. 2004, Pollacco 2005). The SuperWASP setup currently consists of 5 ultra-wide field lens cameras backed by high-quality CCDs, but is designed to hold up to a total of 8 such cameras and CCDs (the upgrade to 8 cameras is expected to be completed in 2005). The photometric precision of the CCDs is largest in the 7–13 mag magnitude range, where it is aimed to be better than 10 mmag (see Kane et al. 2004 for a detailed discussion of the photometric accuracy of the prototype WASPO). Each camera on the SuperWASP setup furthermore has an approximate field of view of  $8^\circ \times 8^\circ$ , so that, accounting for some overlap, the total area covered by 4 cameras operating simultaneously in a rectangular configuration is about  $15^\circ \times 15^\circ$ . The total field of view for the full 8-camera setup will be  $30^\circ \times 15^\circ$ . The large field of view is expected to yield precise photometry of approximately 5 000 to 10 000 stars at a time per operational camera, and thus 40 000 to 80 000 stars at a time for 8 cameras operating simultaneously.

In the following sections, we study in some detail the relative numbers and types of eclipsing binaries detectable in the idealised SuperWASP survey and examine their dependence on the initial mass ratio or secondary mass distribution. By considering the ratio of the number of detectable eclipsing binaries to the number of detectable single stars we also investigate if some regions in the Galaxy are expected to produce more false planetary detections due to eclipsing binaries than others. Our method of calculation is outlined in some detail in Section 2, while the results are presented in Sections 3 and 4. The final section is devoted to concluding remarks.

## 2 METHOD

### 2.1 Eclipsing binaries detectable by SuperWASP

As mentioned in the introduction, each camera on the SuperWASP fork mount is capable of simultaneously monitoring several thousands of 7–13 mag stars with a photometric precision better than

10 mmag. In order to incorporate these instrument characteristics in a binary population synthesis code, a transition needs to be made from bolometric luminosities obtained from stellar evolution calculations to apparent visual magnitudes seen by an observer. We make this transition in the following steps.

First, we determine the absolute visual magnitudes  $M_{V,1}$  and  $M_{V,2}$  of the binary components from their bolometric luminosities  $L_1$  and  $L_2$  as

$$M_{V,i} = -2.5 \log \frac{L_i}{L_\odot} - BC_i + M_{\text{bol},\odot}, \quad i = 1, 2, \quad (1)$$

where  $BC_i$  is the bolometric correction of component  $i$ , and  $M_{\text{bol},\odot} = 4.76$  mag is the bolometric magnitude of the Sun. For stars with a hydrogen-rich envelope, the bolometric correction is determined from the effective temperature by means of polynomial fits to the empirical  $BC-T_{\text{eff}}$  relations given by Flower (1996)<sup>1</sup>. For naked helium stars and white dwarfs, the bolometric correction is assumed to be equal to -5.0 (Smith, Meynet & Mermilliod 1994).

Secondly, we define the visual luminosity  $L_{V,i}$  of component  $i$  as

$$\frac{L_{V,i}}{L_\odot} = 10^{-(M_{V,i} - M_{V,\odot})/2.5}, \quad (2)$$

where  $M_{V,\odot}$  is the absolute visual magnitude of the Sun. For consistency, we determine  $M_{V,\odot}$  from Eq. (1) using the same  $BC-T_{\text{eff}}$  relations as used to determine  $M_{V,1}$  and  $M_{V,2}$ . It follows that  $M_{V,\odot} = 4.84$  mag<sup>2</sup>. The added luminosity of both binary components then gives rise to an absolute visual binary magnitude

$$M_{V,\text{binary}} = M_{V,\odot} - 2.5 \log \frac{L_{V,1} + L_{V,2}}{L_\odot}. \quad (3)$$

Thirdly, we determine the apparent visual magnitude of the binary as

$$m_{V,\text{binary}} = M_{V,\text{binary}} + 5 \log_{10}(d/\text{pc}) - 5 + A_V(d, l, b). \quad (4)$$

Here  $d$  is the distance of the binary from the Sun,  $l$  and  $b$  are the binary's heliocentric Galactic longitude and latitude, and  $A_V(d, l, b)$  is the apparent increase in the visual magnitude of the binary caused by interstellar extinction along the line-of-sight. We incorporate the dependence of  $A_V$  on  $d$ ,  $l$ , and  $b$  in the calculations by means of the extinction model of Hakkila (1997). The model combines the results of several independent extinction studies and also corrects some of the systematic biases these studies are subjected to (see Hakkila 1997 for details and references).

Fourthly, during an eclipse, the apparent visual magnitude of an eclipsing binary increases by

$$\Delta m_{V,\text{binary}} = -2.5 \log \left( 1 - \frac{\Delta L_V}{L_{V,1} + L_{V,2}} \right), \quad (5)$$

where  $\Delta L_V$  is the decrease of the total visual luminosity  $L_{V,1} + L_{V,2}$ . If the radius  $R_1$  of the primary is larger than the radius  $R_2$  of the secondary, the decrease in luminosity during a *total* eclipse is given by

<sup>1</sup> Corrections to the erroneous fits in Table 6 of Flower (1996) were kindly provided by Pasi Nurmi and Henri Boffin (see also Nurmi & Boffin 2003)

<sup>2</sup> This is slightly larger than the usual  $M_{V,\odot} = 4.83$  mag due to the adopted  $M_{\text{bol},\odot}$  and  $BC-T_{\text{eff}}$  relations which yield  $BC_\odot = -0.0778$ . Since this affects the distance to which a star of a given magnitude is visible by less than 0.5%, the adopted  $M_{V,\odot}$  does not significantly affect any of the results presented in this investigation.

$$\Delta L_V = \max \left[ \left( \frac{R_2}{R_1} \right)^2 L_{V,1}, L_{V,2} \right]. \quad (6)$$

The decrease in luminosity for  $R_2 > R_1$  is obtained by exchanging the indices "1" and "2" in Eq. (6). Note that both  $\Delta L_V$  and  $\Delta m_{V,\text{binary}}$  are defined as positive quantities.

## 2.2 The Galactic disc model

The stellar and binary content of the Galaxy are usually modelled by superpositions of density laws describing different Galactic components such as the bulge, the disc, and the halo (see, e.g., Bahcall 1986 for a review). For the purpose of this investigation, we only consider the dominant component made up by the Galactic disc, which we model by means of a stellar distribution law of the form

$$n(R, z) = n_0 \exp\left(-\frac{R}{h_R}\right) \exp\left(-\frac{|z|}{h_z}\right). \quad (7)$$

Here,  $n_0$  is a normalisation constant,  $R$  and  $z$  are the disc's natural cylindrical coordinates,  $h_R$  is the disc's scale length, and  $h_z$  is its scale height. We normalise the distribution to unity by setting  $n_0 = 1/(4\pi h_z h_R^2)$ .

Gilmore & Reid (1983) pointed out that star counts towards the Southern Galactic pole were not well fitted by a single vertical exponential, but that a good agreement could be obtained when two such exponentials, representing the so-called thin and thick disc, with different scale heights were considered. The thin disc has a scale height of about 300 pc and dominates up to  $z \approx 1$  kpc. Its stars cover a wide range of stellar ages between 0 and 10 Gyr. The properties of the thick disc, on the other hand, are less well constrained. They are often referred to as "intermediate" between those of the Galactic disc and the Galactic halo. In particular, the abundances of thick disc stars point towards a moderately metal-poor stellar population. A more extreme metal-weak thick disc, possibly being the tail of the thick disc, also exists, but its contribution to the structure and the content of the Galactic disc is much smaller than that of the thin and thick disc. Hence, as a first approximation, we here only consider binaries with solar metallicity component stars. Estimates for the scale height of the thick disc range from 500 to 1500 pc (e.g. Norris 1999, Du et al. 2003; and references therein). Much larger scale heights have also been claimed, but seem to be ruled out by recent scale height determinations from HST photometry (Kerber, Javiel & Santiago 2001) and 2MASS data (Ojha 2001, Cabrera-Lavers, Garzón, & Hammersley 2005). The age of the thick disc is furthermore thought to be in the range of 12-15 Gyr, so that it is relatively old in comparison to the thin disc.

Observations supporting a large spread in the thick disc's age comparable to that of the thin disc, or the existence of an age gap between the thin and thick disc have so far been inconclusive (Liu & Chaboyer 2000). We therefore assume that the Galactic disc consists of a thin and thick component which originate from different non-overlapping star formation epochs and that the thin disc formed immediately after the thick disc. The total age of the disc is assumed to be 13 Gyr. Binaries formed during the last 10 Gyr of star formation in the Galactic disc are distributed according to a double exponential with  $h_R = 2.8$  kpc and  $h_z = 300$  pc, while binaries formed between 10 Gyr and 13 Gyr ago are distributed according to a double exponential with  $h_R = 3.7$  kpc and  $h_z = 1$  kpc. This gives rise to

- (i) a population of stars with ages between 0 and 10 Gyr and a

relatively small vertical scale height, representative of the thin disc stars, and

- (ii) a population of stars with ages of 10–13 Gyr and a much larger vertical scale height, representative of the thick disc stars.

Hence, over a time span of 13 Gyr, we form 10/3 times more stars in the thin disc than in the thick disc. As we show, below these star formation histories and the adopted thin and thick distributions given by Eq. (7) result in stellar densities in the thin and thick Galactic disc that are compatible with current observational estimates (e.g. Norris 2001). For more details on the adopted scale lengths and scale heights, we refer to Kerber et al. (2001), Ojha (2001), Siegel et al. (2003), and Du et al. (2003).

## 2.3 Binary population synthesis

We use the BiSEPS binary population synthesis code described by Willems & Kolb (2002, 2004) to construct present-day populations of eclipsing binaries in the Galactic disc detectable by the idealised SuperWASP survey. We recall that single star evolution is treated using the formulae derived by Hurley, Pols & Tout (2000), binary orbits are assumed to be circular, and rotational angular velocities are kept synchronised with the orbital motion at all times. Orbital angular momentum losses via gravitational radiation and/or magnetic braking are taken into account as in Hurley, Tout & Pols (2002), and Roche-lobe overflow is treated as in Willems & Kolb (2004). All calculations presented in this paper are furthermore based on the binary evolution parameters corresponding to the standard model (model A) of Willems & Kolb (2004).

The evolution of a large number of binaries consisting of two zero-age main-sequence components was followed up to a maximum evolutionary age of 13 Gyr. The initial primary and secondary masses,  $M_1$  and  $M_2$ , are taken from a grid of 50 logarithmically spaced masses in the interval between 0.1 and 20  $M_\odot$ , and the initial orbital periods,  $P_{\text{orb}}$ , from a grid of 250 logarithmically spaced periods in the interval between 0.1 and 10 000 days. In order to avoid spurious spikes in the distribution functions of simulated binaries, each grid point is actually randomly offset from the center of the grid cells according to uniform  $\log M_1$ ,  $\log M_2$ , and  $\log P_{\text{orb}}$  distributions within the boundaries of the grid cells (cf. Hurley et al. 2002). For symmetry reasons only binaries with  $M_1 > M_2$  are evolved. At the end of the calculation of each binary sequence, the evolutionary track is scanned for phases where *total* eclipses would be detectable by SuperWASP. We furthermore only retain binaries that are detached or in a thermally and dynamically stable mass-transfer phase. In view of the generally short life time of thermal and dynamical time scale mass-transfer episodes, we do not expect this limitation to significantly affect our results.

The statistical contribution of a binary to the population of eclipsing binaries detectable by SuperWASP is determined by the probability distribution functions of the initial binary parameters, the adopted star formation rate, the fraction of stars in binaries, the position of the binary in the Galactic disc, and the probability that the orbit is oriented suitably for the observation of total eclipses. We assume the initial primary masses to be distributed according to an initial mass function (IMF) with a slope of -1.3 for  $0.1 M_\odot \leq M_1 < 0.5 M_\odot$ , -2.2 for  $0.5 M_\odot \leq M_1 < 1.0 M_\odot$ , and -2.7 for  $1.0 M_\odot \leq M_1$ . We furthermore assume that the distribution of initial orbital separations is logarithmically flat, such that  $\chi(\log a) = 0.078636$  for  $3 \leq a/R_\odot \leq 10^6$ . The initial mass ratio distribution is parametrized as  $n(q) \propto q^s$  with  $s \in \mathbb{R}$  a free parameter and  $0 < q = M_2/M_1 \leq 1$ , though we also investigate

**Table 1.** Idealised transit survey characteristics.

model	magnitude range	photometric precision (mag)
1	7–13	0.01
2	7–15	0.01
3	7–13	0.1
4	7–15	0.1

the case where both binary components are picked independently from the same IMF (see Willems & Kolb 2002 for details and references). We furthermore assume that 50% of all stars are binaries and that the Galactic star-formation rate has been constant for the past 13 Gyr. The star-formation is calibrated so that one binary or single star with  $M_1 > 0.8 M_\odot$  is born in the Galaxy each year, in concordance with the observationally inferred birthrate of Galactic white dwarfs (Weidemann 1990).

The role of the position of the binary in the Galactic disc is taken into account by means of Eqs. (4) and (7). More specifically, for a given absolute visual magnitude  $M_{V,\text{binary}}$  and a given set of Galactic coordinates  $(l, b)$ , Eq. (4) translates the optimal SuperWASP magnitude range  $7 \text{ mag} \leq m_{V,\text{binary}} \leq 13 \text{ mag}$  into a range of optimal distances  $d_{\min} \leq d \leq d_{\max}$ . Since the translation depends on the interstellar extinction coefficient  $A_V(d, l, b)$ , which itself is a function of the distance  $d$  of the binary from the Sun, the optimal distance range has to be determined iteratively. The dependence of  $A_V$  on the Galactic longitude and latitude furthermore implies that  $d_{\min}$  and  $d_{\max}$  are also functions of  $l$  and  $b$ . The statistical weight of a binary with Galactic coordinates  $(l_0, b_0)$  is then determined by (i) integrating Eq. (7) over all distances  $d$  ranging from  $d_{\min}$  to  $d_{\max}$ , and (ii) integrating the resulting two-dimensional function of  $l$  and  $b$  over a rectangular field of view centred on  $(l_0, b_0)$ . To this end, the Galactocentric cylindrical coordinates  $(R, z)$  appearing in Eq. (7) are expressed in terms of the Heliocentric spherical coordinates  $(d, l, b)$  as

$$\left. \begin{aligned} R &= \left( d^2 \cos^2 b - 2dR_\odot \cos b \cos l + R_\odot^2 \right)^{1/2}, \\ z &= d \sin b + z_\odot. \end{aligned} \right\} \quad (8)$$

Here  $R_\odot$  is the distance of the projection of the Sun on the Galactic plane to the Galactic centre, and  $z_\odot$  is the height of the Sun above the Galactic plane. We here adopt the values  $R_\odot = 8.5 \text{ kpc}$  and  $z_\odot = 30 \text{ pc}$  (e.g. Binney & Tremaine 1987; Reid 1993; Chen et al. 2001; and references therein).

The probability to observe binary eclipses, finally, is determined by the radii of the component stars and the orbital separation. In particular, two binary components with radii  $R_1$  and  $R_2$  separated by a distance  $a$ , will show total eclipses for orbital inclinations  $i \geq i_0$ , with  $i_0$  determined by

$$\cos i_0 = \frac{|R_1 - R_2|}{a}. \quad (9)$$

Adopting a uniform distribution for the cosine of the orbital inclination  $i$  then gives an eclipse probability given by

$$P(i \geq i_0) = \int_{i_0}^{\pi/2} \sin i \, di = \frac{|R_1 - R_2|}{a}. \quad (10)$$

### 3 GALACTIC DISTRIBUTIONS

We used the technique and the assumptions outlined in the previous section to construct Galactic distributions of eclipsing binaries and

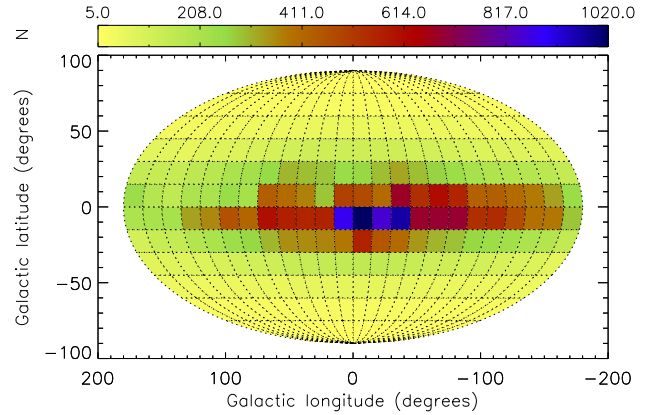


**Figure 1.** Distribution of the number  $N$  of eclipsing binaries detectable in the Galactic disc, for survey model 1 and a flat initial mass ratio distribution  $n(q) = 1$ . Note that the color scale for  $N$  is linear.

single stars detectable by an idealised SuperWASP survey. Specifically, we adopt four different idealised transit survey characteristics. In survey model 1 (our standard survey model), the magnitude range and eclipse detection threshold are assumed to be 7–13 mag and 0.01 mag, respectively. The assumptions adopted in the other three survey models are summarised in Table 1. We note that the eclipse detection threshold is irrelevant for single stars, so that models 3 and 4 are equivalent to models 1 and 2 for these stars.

The Galactic distribution of eclipsing binaries detectable by SuperWASP is shown in Fig. 1, for survey model 1 and a flat initial mass ratio distribution  $n(q) = 1$ . The systems are grouped in  $15^\circ \times 15^\circ$  bins in Galactic longitude and latitude, corresponding approximately to the combined field of view of four SuperWASP cameras operating simultaneously in a rectangularly mounted configuration. The double exponential distribution functions adopted for the thin and thick Galactic disc components yield a strong concentration of systems towards the Galactic plane ( $b = 0^\circ$ ) and towards the Galactic centre ( $l = 0^\circ, b = 0^\circ$ ). The asymmetry in the distributions with respect to the Galactic centre is caused by the Galactic longitude and latitude dependency of the interstellar extinction model [see, e.g., Fig. 11 in Hakkila et al. (1997)]. The largest number of systems is found in the  $15^\circ \times 15^\circ$  field of view centred on  $(l, b) = (-7.5^\circ, -7.5^\circ)$ . The behaviour of the distributions of detectable eclipsing binaries for the other three survey models is similar to that of model 1. The same applies to the Galactic distributions of single stars detectable by SuperWASP.

The contributions of the thin and thick Galactic disc to the population of eclipsing binaries detectable by SuperWASP are shown separately in Fig. 2. The thin disc component contains approximately 96% of the sample of detectable eclipsing binaries (see Section 4). The fine structure in the thick disc component reflects the variations of the interstellar extinction as a function of Galactic longitude and latitude. These variations are more apparent for the thick Galactic disc than for the thin Galactic disc because it is much less centrally condensed.

In Fig. 3, we show the variation of the ratio  $R$  of the number of eclipsing binaries to the number of single stars detectable by SuperWASP as a function of Galactic longitude and latitude, in the case of survey model 1 and a flat initial mass ratio distribution. The ratio is largest for the bin centred on  $(l, b) = (-7.5^\circ, -22.5^\circ)$ , so that this region is less favourable for SuperWASP if false exoplanet

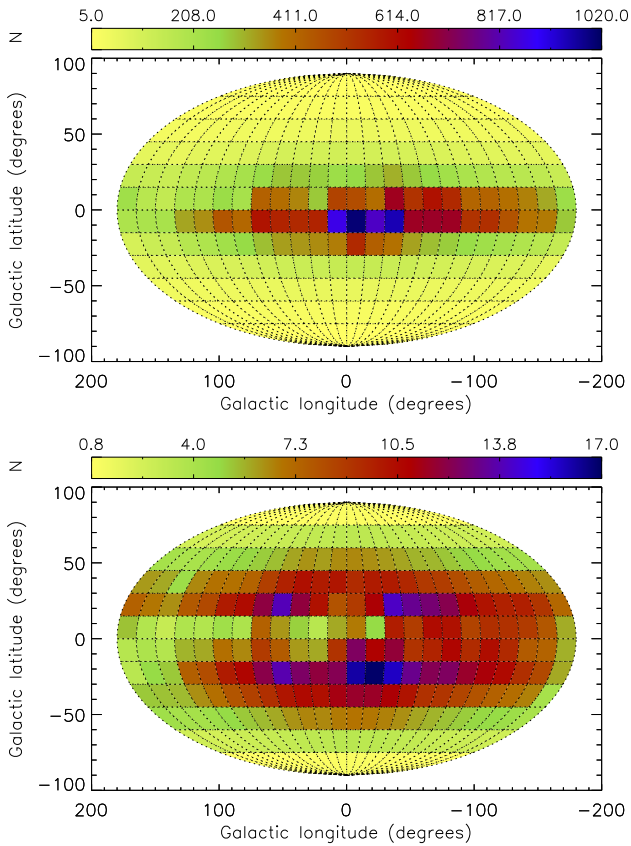


**Figure 2.** As Fig. 1, but with the Galactic disc separated into its thin (top panel) and thick (bottom panel) components.

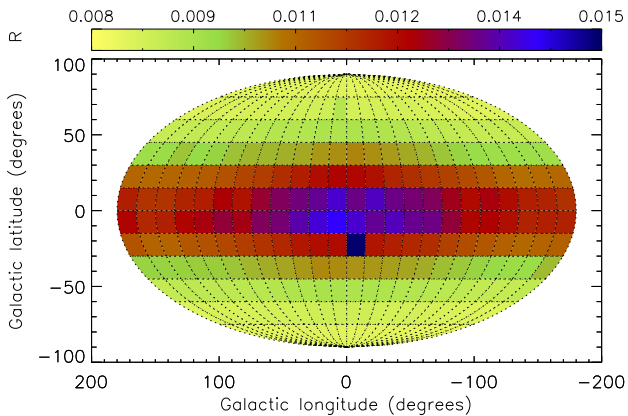


**Figure 3.** As Fig. 1, but in units of the number of detectable single stars.

transit detections due to eclipsing binaries are to be minimized. This fairly localized peak in the distribution of  $R$  is already apparent as a local maximum in  $l$  direction in Fig. 1. The peak results from the interplay between a decrease in the interstellar extinction in this bib (see Fig. 11 in Hakkila 1997) and the non-trivial differential behaviour between single and binary stars to the interstellar extinction (binaries emit the combined light of two stars, affecting the distance to which they are observable). For  $75^\circ \lesssim l \lesssim 285^\circ$ , more favourable regions are found at any Galactic latitude between

$0^\circ$  and  $90^\circ$ , while for  $l \lesssim 75^\circ$  and  $l \gtrsim 285^\circ$  more favourable regions are located at Galactic latitudes  $|b| \gtrsim 15^\circ$  (except for the bin centred on  $l = -7.5^\circ$  and  $b = -22.5^\circ$ ). The same holds true for survey models 2–4. In all models, the ratio  $R$  varies across the sky by less than a factor of 2.5.

#### 4 ABSOLUTE AND RELATIVE NUMBERS

In the previous Section, we have seen that the distribution of eclipsing binaries and single stars detectable by an idealised SuperWASP survey in the Galactic disc is similar for all four survey models listed in Table 1. In this section we show the effect of the model assumptions on the number of detectable eclipsing binaries and single stars, and on their breakdown in subgroups according to the type of stars involved.

The total number of detectable eclipsing binaries and single stars is listed in Table 2, for each of the four survey models considered and for different initial mass ratio or initial secondary mass distributions. For survey model 1 and a flat initial mass ratio distribution  $n(q) = 1$ , the number of eclipsing binaries is of the order of  $4 \times 10^4$ . Extending the detectable magnitude range from 7–13 mag (model 1) to 7–15 mag (model 2) increases the total number of systems by approximately a factor of 4. Increasing the minimum detectable eclipse depth from 0.01 mag (model 1) to 0.1 mag (model 3), on the other hand, yields a decrease of the total number of systems by about a factor of 2. The initial mass ratio or secondary mass distribution has a significant effect on the absolute number of systems only when small initial mass ratios  $M_2/M_1$  are favoured: when  $n(q) \propto q^{-0.99}$  the number of detectable eclipsing binaries decreases by approximately a factor of 50 compared to the case of  $n(q) = 1$ . The dominance of extreme-mass ratio systems implies a large number of undetectable small-amplitude eclipses.

The total number of detectable single stars is typically more than two orders of magnitude larger than the total number of detectable eclipsing binaries in the same survey model (the ratio of the number of detectable eclipsing binaries to the number of detectable single stars is listed in the last column of Table 2). In the case of the initial mass ratio distribution  $n(q) \propto q^{-0.99}$ , the difference even amounts to three to four orders of magnitude, depending on the adopted survey model. The dominance of single stars is partly because eclipsing binaries are subjected to the additional observational threshold that their eclipses must be deep enough to be observable and identifiable by the transit survey, and partly because the presence of a companion can alter the life time and evolutionary path of a binary component in comparison to those of a single star. Mass transfer, e.g., can strip a red giant down to its core, leaving behind a rapidly dimming white dwarf which is less likely to be detected than its giant progenitor. We also note that the number of detectable eclipsing binaries given in Table 2 is by no means representative of the total number of binaries seen by the survey since the latter includes eclipsing systems with undetectable eclipse amplitudes as well as non-eclipsing binaries.

In Table 3, the population of detectable single stars is subdivided according to the type of star and according to their membership to the thin or thick Galactic disc. Approximately 60% of all single stars in the magnitude range between 7 and 13 mag (model 1) are main-sequence stars, 20% are horizontal-branch stars, and 10% are giant-branch stars, 2% are Hertzsprung-gap stars, 1% are asymptotic giant branch stars, and 1% are white dwarf stars. If the detectable magnitude range is extended from 7–13 mag to 7–15 mag (model 2), the relative number of horizontal branch stars decreases

**Table 2.** The total number of eclipsing binaries and single stars detectable by an idealised SuperWASP survey, for each of the four survey models listed in Table 1 and for different initial mass ratio or initial secondary mass distributions. The last column in the table lists the ratio of the total number of detectable eclipsing binaries to the total number of detectable single stars.

model	eclipsing binaries	single stars	ratio
$n(q) \propto q, 0 < q \leq 1$			
1	$4.8 \times 10^4$	$3.7 \times 10^6$	$1.3 \times 10^{-2}$
2	$2.0 \times 10^5$	$1.8 \times 10^7$	$1.1 \times 10^{-2}$
3	$2.4 \times 10^4$	$3.7 \times 10^6$	$6.5 \times 10^{-3}$
4	$1.0 \times 10^5$	$1.8 \times 10^7$	$5.6 \times 10^{-3}$
$n(q) = 1, 0 < q \leq 1$			
1	$4.3 \times 10^4$	$3.7 \times 10^6$	$1.2 \times 10^{-2}$
2	$1.8 \times 10^5$	$1.8 \times 10^7$	$1.0 \times 10^{-2}$
3	$1.8 \times 10^4$	$3.7 \times 10^6$	$4.9 \times 10^{-3}$
4	$7.9 \times 10^4$	$1.8 \times 10^7$	$4.4 \times 10^{-3}$
$n(q) \propto q^{-0.99}, 0 < q \leq 1$			
1	$1.1 \times 10^3$	$3.7 \times 10^6$	$3.0 \times 10^{-4}$
2	$4.9 \times 10^3$	$1.8 \times 10^7$	$2.7 \times 10^{-4}$
3	$3.0 \times 10^2$	$3.7 \times 10^6$	$8.1 \times 10^{-5}$
4	$1.4 \times 10^3$	$1.8 \times 10^7$	$7.8 \times 10^{-5}$
$M_2$ from same IMF as $M_1$			
1	$3.2 \times 10^4$	$3.7 \times 10^6$	$8.6 \times 10^{-3}$
2	$1.5 \times 10^5$	$1.8 \times 10^7$	$8.3 \times 10^{-3}$
3	$4.6 \times 10^3$	$3.7 \times 10^6$	$1.2 \times 10^{-3}$
4	$2.5 \times 10^4$	$1.8 \times 10^7$	$1.4 \times 10^{-3}$

**Table 3.** Contributions of different types of stars in the thin and thick Galactic disc to the population of detectable single stars, for survey models 1 and 2. In column 1, MS stands for main sequence, HG for Hertzsprung gap, GB for giant branch, HB for horizontal branch, AGB for asymptotic giant branch, and WD for white dwarf.

stellar type	model 1		model 2	
	thin disc	thick disc	thin disc	thick disc
MS	60.76%	0.78%	64.83%	1.91%
HG	1.70%	0.17%	1.85%	0.36%
GB	9.84%	2.61%	8.17%	3.77%
HB	20.02%	1.92%	13.87%	1.89%
AGB	0.96%	0.10%	0.66%	0.09%
WD	1.00%	0.14%	2.22%	0.38%
Total	94.28%	5.72%	91.60%	8.40%

somewhat, while the relative numbers of main-sequence and white dwarf stars increases. The ratio of the number of detectable single stars in the thin Galactic disc to the number of detectable single stars in the thick Galactic disc is approximately 15 to 1 for survey model 1 and 10 to 1 for survey model 2, comparable to current estimates for the ratio of stellar densities in the thin and thick Galactic disc (e.g. Norris 2001).

Table 4 gives a detailed breakdown into types of binaries that make up the sample of eclipsing binaries detectable by the transit survey. In the case of survey model 1, the dependence of the relative contributions of different types of systems on the adopted initial

mass ratio or initial secondary mass distribution is visualized in Fig. 4.<sup>3</sup>

The dominant group of detectable eclipsing binaries consists of two detached main-sequence stars. In the case of survey model 1 and a flat initial mass ratio distribution, this subgroup of systems accounts for 60% of the population of detectable eclipsing binaries. Detached giant-branch main-sequence star binaries account for approximately 20% of the population, detached horizontal-branch main-sequence star binaries for approximately 10%, and Hertzsprung-gap main-sequence star binaries for about 2%. Other types of binaries contribute at most 1%. The relative number of detached double main-sequence star binaries increases to 65% for survey model 2 and 70–80% for survey models 3 and 4. The contribution of giant-branch main-sequence star binaries, on the other hand, decreases from 20% in survey models 1 and 2 to 5% in survey models 3 and 4. The relative number of detectable eclipsing binaries in the thin Galactic disc furthermore varies from 93% and 99% between the different survey models considered. In addition, it is interesting to note that the most abundant group of eclipsing binaries detectable by the transit survey model in the thick Galactic disc consists of detached giant-branch main-sequence star binaries. This is because essentially all former double main-sequence stars with large-amplitude eclipses have evolved off the main sequence in the thick disc population.

In the case of the initial mass ratio distribution  $n(q) \propto q$ , the relative contribution of detached double main-sequence star binaries decreases in favour of detached giant-branch main-sequence star and horizontal branch main-sequence star binaries. The numbers for the initial mass ratio distribution  $n(q) \propto q^{-0.99}$  show the opposite effect. The largest shifts in the relative contributions occur when the secondary mass is assumed to be distributed independently according to the same IMF as the primary mass. In particular, the contribution of detached double main-sequence star binaries then increases to 80–90%, while the contribution of detached asymptotic giant-branch main-sequence star binaries decreases to 5–10% (see Fig. 4).

## 5 CONCLUSIONS

In this exploratory study we used the BiSEPS binary population synthesis code to estimate the number of eclipsing binaries and single stars detectable in the Galactic disc by an idealised SuperWASP exoplanet transit survey. The Galactic disc is modeled by a superposition of a young (thin) and old (thick) component, both of which are described by means of a double exponential distribution function characterised by different scale lengths and scale heights. The models yield a strong concentration of eclipsing binaries and single stars towards the Galactic plane and the Galactic centre.

The ratio of the number of detectable eclipsing binaries to the number of detectable single stars varies by less than a factor of 2.5 across the sky. It is largest in the direction of the Galactic longitude  $l = -7.5^\circ$  and the Galactic latitude  $b = -22.5^\circ$ , so that the number of false exoplanet transit detections due to eclipsing binaries can be expected to be largest in this direction. More favourable regions on the sky aimed at minimizing false planetary detections are therefore located away from this area. The best conditions are

<sup>3</sup> Note that Kolb & Willems (2004) presented early results of these simulations. The fractions in their Table 2 are now superseded by the results presented here.

**Table 4.** Contributions of the most common types of binaries in the thin and thick Galactic disc to the population of eclipsing binaries detectable by an idealised SuperWASP survey, for each of the survey models listed in Table 1 and different initial mass ratio or initial secondary mass distributions. In column 1, MS stands for main sequence, HG for Hertzsprung gap, GB for giant branch, HB for horizontal branch, AGB for asymptotic giant branch, nHe for naked helium star, and WD for white dwarf. Detached and semi-detached systems are indicated in column 2 by the labels D and SD, respectively.

binary components	binary type	model 1		model 2		model 3		model 4	
		thin disc	thick disc	thin disc	thick disc	thin disc	thick disc	thin disc	thick disc
$n(q) \propto q, 0 < q \leq 1$									
MS+MS	D	46.72%	0.22%	50.05%	0.62%	67.30%	0.35%	70.93%	0.94%
HG+MS	D	1.53%	0.11%	1.76%	0.28%	1.75%	0.14%	1.92%	0.33%
GB+MS	D	25.30%	4.99%	22.88%	7.66%	7.40%	0.61%	7.02%	1.18%
GB+HG/GB/HB	D	1.72%	0.27%	1.46%	0.35%	1.80%	0.42%	1.52%	0.52%
HB+MS	D	15.06%	0.06%	11.56%	0.07%	15.04%	0.00%	11.51%	0.00%
AGB+MS	D	1.20%	0.01%	0.92%	0.01%	0.42%	<0.01%	0.31%	<0.01%
AGB+HG/GB/HB	D	0.26%	0.01%	0.20%	0.01%	0.41%	<0.01%	0.31%	<0.01%
nHe+MS	D	0.18%	0.00%	0.14%	0.00%	0.04%	0.00%	0.03%	0.00%
WD+MS	D	0.13%	0.02%	0.25%	0.05%	0.08%	0.01%	0.15%	0.03%
MS+MS	SD	0.65%	<0.01%	0.53%	<0.01%	1.30%	<0.01%	1.02%	<0.01%
HG+MS	SD	0.12%	<0.01%	0.10%	<0.01%	0.23%	<0.01%	0.19%	<0.01%
GB+MS	SD	0.91%	0.01%	0.73%	0.01%	1.81%	0.02%	1.41%	0.03%
HB+MS	SD	0.11%	0.00%	0.06%	0.00%	0.15%	0.00%	0.09%	0.00%
Other		0.40%	0.01%	0.30%	<0.01%	0.73%	<0.01%	0.56%	<0.01%
Total		94.29%	5.71%	90.94%	9.06%	98.46%	1.54%	96.97%	3.03%
$n(q) = 1, 0 < q \leq 1$									
MS+MS	D	60.58%	0.27%	63.33%	0.74%	73.55%	0.38%	76.55%	1.01%
HG+MS	D	1.56%	0.12%	1.79%	0.28%	1.49%	0.12%	1.61%	0.27%
GB+MS	D	17.71%	3.28%	15.85%	5.03%	5.64%	0.44%	5.25%	0.84%
GB+HG/GB/HB	D	0.98%	0.15%	0.81%	0.19%	1.22%	0.28%	1.01%	0.34%
HB+MS	D	12.17%	0.04%	9.12%	0.04%	12.24%	0.00%	9.19%	0.00%
AGB+MS	D	0.91%	0.01%	0.68%	0.01%	0.33%	<0.01%	0.24%	<0.01%
AGB+HG/GB/HB	D	0.15%	0.01%	0.11%	<0.01%	0.29%	<0.01%	0.21%	<0.01%
nHe+MS	D	0.14%	0.00%	0.10%	0.00%	0.05%	0.00%	0.04%	0.00%
WD+MS	D	0.29%	0.04%	0.57%	0.11%	0.27%	0.04%	0.53%	0.10%
MS+MS	SD	0.52%	<0.01%	0.41%	<0.01%	1.24%	<0.01%	0.95%	<0.01%
HG+MS	SD	0.09%	<0.01%	0.08%	<0.01%	0.22%	<0.01%	0.17%	<0.01%
GB+MS	SD	0.66%	0.01%	0.52%	0.01%	1.58%	0.01%	1.20%	0.02%
HB+MS	SD	0.08%	0.00%	0.04%	0.00%	0.12%	0.00%	0.07%	0.00%
Other		0.24%	<0.01%	0.17%	0.01%	0.49%	<0.01%	0.39%	0.01%
Total		96.08%	3.92%	93.58%	6.42%	98.73%	1.27%	97.41%	2.59%

found at Galactic longitudes  $75^\circ \lesssim l \lesssim 285^\circ$  and, for Galactic longitudes  $|l| \lesssim 75^\circ$ , at Galactic latitudes  $|b| \gtrsim 15^\circ$ .

Depending on the adopted survey model, the total number of single stars in the magnitude range detectable by the idealised SuperWASP survey is of the order of  $10^6$ – $10^7$ . The total number of detectable eclipsing binaries varies from a few times  $10^2$ – $10^5$ , with the exact number depending on the adopted survey model (limiting magnitude and eclipse amplitude) and on the initial mass ratio or initial secondary mass distribution. In view of the large number of stars and binaries observed by SuperWASP each night, the lower end of the predicted number of eclipsing binaries (resulting from the initial mass ratio distribution  $n(q) \propto q^{-0.99}$ ) could soon be confronted with interesting and potentially stringent observational constraints, assuming that our simplifications still capture the essence of the real SuperWASP set-up.

Provided that complete samples of the most abundant types of binaries can be compiled by SuperWASP, the relative contribution of each type of binary to the total population can be used to further constrain the initial mass ratio or initial secondary mass distribution (see Fig. 4). In particular, for our standard survey model, the rela-

tive number of double main-sequence star binaries increases from 45% in the case of the initial mass ratio distribution  $n(q) \propto q$  to 80% in the case of the initial mass ratio distribution  $n(q) \propto q^{-0.99}$ , and 90% in the case where the initial secondary mass is distributed independently according to the same IMF as the primary mass. The contribution of white dwarf main-sequence star binaries increases from 0.1% in the case of the initial mass ratio distribution  $n(q) \propto q$  to 0.7% in the case of the initial mass ratio distribution  $n(q) \propto q^{-0.99}$ , and 1.3% in the case where the initial secondary mass is distributed independently according to the same IMF as the primary mass. In contrast, the relative contributions of the other major groups of binaries tend to decrease when the initial mass ratio distribution is changed from  $n(q) \propto q$  to  $n(q) \propto q^{-0.99}$  or an independent initial secondary mass distribution. Similar diagnostics for the initial mass ratio or initial secondary mass distribution can be obtained by considering ratios of numbers of different types of eclipsing binaries detectable by the transit survey rather than their fractional contributions to the total population.

In view of the large variety of eclipsing binaries found, we did not consider the effects of varying some of the binary evo-



Table 4 – *continued*

binary components	binary type	model 1		model 2		model 3		model 4	
		thin disc	thick disc	thin disc	thick disc	thin disc	thick disc	thin disc	thick disc
$n(q) \propto q^{-0.99}, 0 < q \leq 1$									
MS+MS	D	78.11%	0.31%	78.75%	0.82%	79.53%	0.41%	80.90%	1.07%
HG+MS	D	1.36%	0.11%	1.53%	0.25%	1.16%	0.09%	1.23%	0.21%
GB+MS	D	8.86%	1.53%	7.86%	2.35%	3.88%	0.29%	3.51%	0.53%
GB+HG/GB/HB	D	0.38%	0.06%	0.31%	0.07%	0.74%	0.17%	0.60%	0.20%
HB+MS	D	7.08%	0.02%	5.40%	0.02%	9.01%	0.00%	6.57%	0.00%
AGB+MS	D	0.49%	<0.01%	0.35%	<0.01%	0.23%	<0.01%	0.17%	<0.01%
AGB+HG/GB/HB	D	0.06%	<0.01%	0.04%	<0.01%	0.18%	<0.01%	0.13%	<0.01%
nHe+MS	D	0.08%	0.00%	0.06%	0.00%	0.06%	0.00%	0.04%	0.00%
WD+MS	D	0.65%	0.09%	1.31%	0.25%	1.16%	0.14%	2.26%	0.38%
MS+MS	SD	0.30%	<0.01%	0.22%	<0.01%	1.10%	<0.01%	0.82%	<0.01%
HG+MS	SD	0.05%	<0.01%	0.04%	<0.01%	0.19%	<0.01%	0.15%	<0.01%
GB+MS	SD	0.34%	<0.01%	0.26%	<0.01%	1.26%	0.01%	0.94%	0.01%
HB+MS	SD	0.04%	0.00%	0.02%	0.00%	0.09%	0.00%	0.05%	0.00%
Other		0.09%	<0.01%	0.08%	0.01%	0.30%	<0.01%	0.23%	<0.01%
Total		97.89%	2.11%	96.23%	3.77%	98.89%	1.11%	97.60%	2.40%
$M_2$ from same IMF as $M_1$									
MS+MS	D	88.17%	0.47%	86.83%	1.16%	85.75%	0.91%	83.93%	1.96%
HG+MS	D	1.40%	0.14%	1.53%	0.30%	1.08%	0.13%	1.00%	0.24%
GB+MS	D	5.19%	1.10%	4.47%	1.64%	2.87%	0.32%	2.20%	0.48%
GB+HG/GB/HB	D	0.15%	0.03%	0.11%	0.04%	0.53%	0.17%	0.35%	0.17%
HB+MS	D	1.79%	0.01%	1.22%	0.01%	2.64%	0.00%	1.58%	0.00%
AGB+MS	D	0.11%	<0.01%	0.07%	<0.01%	0.04%	<0.01%	0.03%	<0.01%
AGB+HG/GB/HB	D	0.01%	<0.01%	0.01%	<0.01%	0.05%	<0.01%	0.03%	<0.01%
nHe+MS	D	<0.01%	0.00%	<0.01%	0.00%	0.01%	0.00%	0.01%	0.00%
WD+MS	D	1.11%	0.17%	2.06%	0.42%	3.93%	0.51%	6.26%	1.09%
MS+MS	SD	0.04%	<0.01%	0.03%	<0.01%	0.30%	<0.01%	0.18%	<0.01%
HG+MS	SD	0.01%	<0.01%	0.01%	<0.01%	0.09%	<0.01%	0.07%	<0.01%
GB+MS	SD	0.08%	<0.01%	0.06%	<0.01%	0.58%	0.01%	0.35%	0.01%
HB+MS	SD	<0.01%	0.00%	<0.01%	0.00%	0.01%	0.00%	0.01%	0.00%
Other		0.02%	<0.01%	0.03%	<0.01%	0.06%	0.01%	0.04%	0.01%
Total		98.08%	1.92%	96.43%	3.57%	97.94%	2.06%	96.04%	3.96%

lution parameters as is customary in binary population synthesis studies (see, e.g., Willems & Kolb 2002, 2003, 2004). In particular, the masses and orbital periods of the eclipsing binaries may be affected by uncertainties in the treatment of mass transfer if either of the binary components at some point of its evolution filled its critical Roche lobe. Additional uncertainties affecting the binary separation (and thus the possibility of interactions between the component stars as well as the probability to observe the system as an eclipsing binary) are introduced by uncertainties in systemic orbital angular momentum losses through, e.g., magnetic braking and stellar winds. The latter can furthermore also have a strong impact on the stars themselves, especially during or after evolutionary phases that are accompanied by high wind mass-loss rates such as the giant branch, asymptotic giant branch, and Wolf-Rayet stages of stellar evolution. The impact of these uncertainties on the relative numbers and statistical properties of different types of eclipsing binaries will be addressed in follow-up studies that are tailored more closely to represent the precise properties of different ongoing and future exoplanet transit surveys.

The results of our exploratory study reveal very encouraging differential trends in the collective properties of the eclipsing binary population that can be probed by extrasolar planet transit surveys. This suggests that transit surveys will be able to deliver stringent

constraints on parameters describing the formation and evolution of binaries once statistically meaningful results from such surveys are available. In future applications of this work we will consider a fine-tuned transit survey model that more closely matches the actual parameters of the SuperWASP survey, and that also addresses the fact that the discovery probability of eclipses will depend on the eclipse properties. We will also extend our study to other transit surveys.

#### ACKNOWLEDGEMENTS

We are grateful to Pasi Nurmi and Henri Boffin for providing the corrected fits to the bolometric corrections given by Flower (1996), and Carole Haswell, Andy Norton and Sean Ryan for valuable discussions on the observational aspects of the SuperWASP project. We also thank the referee, Chris Tout, for a constructive report which helped improve the paper. Part of this research was supported by the British Particle Physics and Astronomy Research Council (PPARC). BW acknowledges the support of NASA ATP grant NAG5-13236 to Vicky Kalogera and the hospitality of the Open University which allowed the final stages for this project to



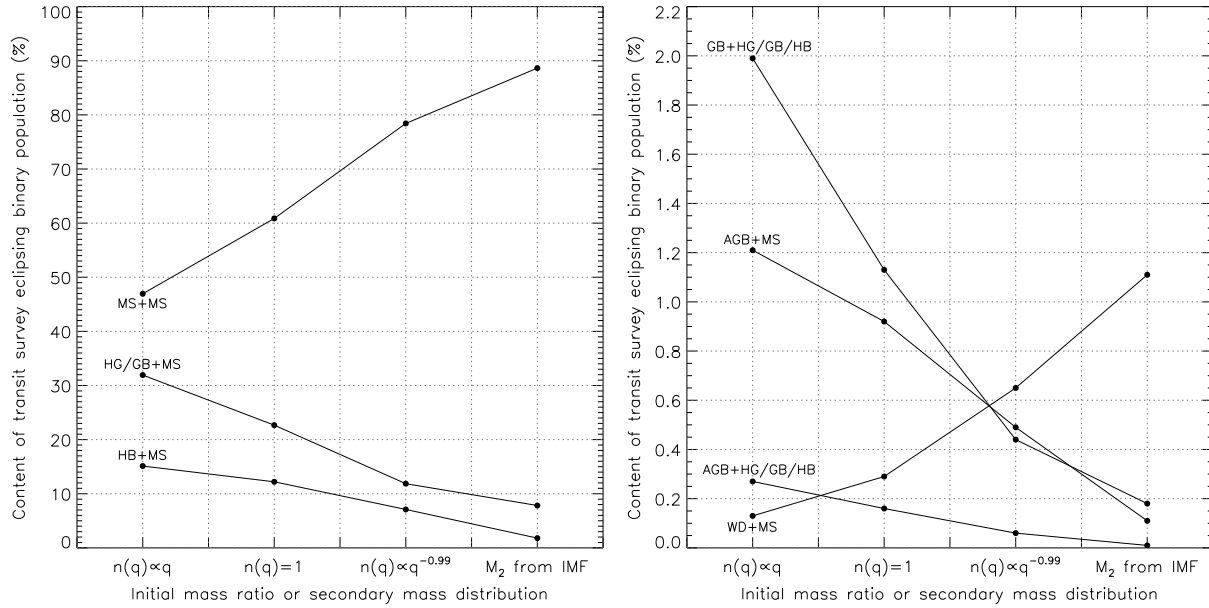


**Figure 4.** Relative contribution of the most common types of binaries to the population of eclipsing binaries detectable by an idealised SuperWASP survey in the (thin and thick) Galactic disc, for survey model 1 and different initial mass ratio or initial secondary mass distributions. The abbreviations MS, HG, GB, ... have the same meaning as in Tables 3 and 4.

be laid out. This research made extensive use of NASA's Astrophysics Data System Bibliographic Services.

## REFERENCES

- Alonso R., et al., 2004, *ApJ*, 613, L153  
 Bahcall J.N., 1986, *ARA&A* 24, 577  
 Binney J., Tremaine S., 1987, *Galactic dynamics*, Princeton University Press  
 Bouchy F., Pont F., Santos N.C., Melo C., Mayor M., Queloz D., Udry S., 2004, *A&A*, 421, L13  
 Brown T.M., 2003, *ApJ* 593, L125  
 Cabrera-Lavers A., Garzón F., Hammersley P.L. 2005, *A&A*, 433, 173  
 Charbonneau D., 2003, *Space Science Reviews*, ISSI Workshop on Planetary Systems and Planets in Systems, Eds. S. Udry, W. Benz and R. von Steiger, Dordrecht: Kluwer, in press  
 Charbonneau D., Brown T.M., Latham D.W., Mayor M., 2000, *ApJ* 529, L45  
 Charbonneau D., Brown T.M., Dunham E.W., Latham D.W., Looper D.L., Mandushev G., 2003, *AIP Conf Proc*, The Search for Other Worlds, Eds. S. S. Holt and D. Deming, in press (astro-ph/0401063)  
 Chen B., et al., 2001, *ApJ* 553, 184  
 Christian D.J., et al. 2004, *Proceedings of the 13th Cool Stars Workshop*, Ed. F. Favata, in press (astro-ph/0411019)  
 Du C., Zhou X., Ma J., Chen A.B., Yang Y., Li J., Wu H., Jiang Z., Chen J., *A&A* 407, 541  
 Flower P.J., 1996, *ApJ* 469, 355  
 Gilmore G., Reid N., 1983, *MNRAS* 202, 1025  
 Hakikila J., Myers J.M., Stidham B.J., Hartmann D.H., 1997, *AJ* 114, 2042  
 Henry G.W., Marcy G.W., Butler R.P., Vogt S.S., 2000, *ApJ* 529, L41  
 Horne K., 2002, *ESA SP-485: Stellar Structure and Habitable Planet Finding*, 137  
 Horne K., 2003, *ASP Conf. Ser. 294: Scientific Frontiers in Research on Extrasolar Planets*, 361  
 Hurley J.R., Pols O.R., Tout C.A., 2000, *MNRAS* 315, 543  
 Hurley J.R., Tout C.A., Pols O.R., 2002, *MNRAS* 329, 897  
 Kane S.R., Horne K., Street R.A., Pollacco D.L., James D., Tsapras Y.,

- Collier Cameron A., 2003, *ASP Conf. Ser. 294: Scientific Frontiers in Research on Extrasolar Planets*, 387  
 Kane S.R., Collier Cameron A., Horne K., James D., Lister T.A., Pollacco D.L., Street R.A., Tsapras Y., 2004, *MNRAS*, 353, 689  
 Kerber L.O., Javiel S.C., Santiago, B.X., 2001, *A&A* 365, 424  
 Konacki M., Torres G., Jha S., Sasselov D.D., 2003, *Nature* 421, 507  
 Konacki M., et al., 2004, *ApJ*, 609, L37  
 Konacki M., Torres G., Sasselov D.D., Jha S., 2005, *ApJ*, 624, 372  
 Kolb U., Willems B., 2004, *RevMexAA* 20, 101  
 Liu W.M., Chaboyer B., 2000, *ApJ* 544, 818  
 Norris J.E., 1999, *Ap&SS* 265, 213  
 Norris J.E., 2001, in *Encyclopedia of Astronomy and Astrophysics*, Ed. P. Murdin, Bristol: IoP Publishing, p 841  
 Nurmi P., Boffin H.M.J., 2003, *A&A* 408, 803  
 Ojha D.K., 2001, *MNRAS* 322, 426  
 Pollacco D., 2005, *Astronomy and Geophysics*, 46, 19  
 Pont F., Bouchy F., Queloz D., Santos N.C., Melo C., Mayor M., Udry S., 2004, *A&A*, 426, L15  
 Reid M.J., 1993, *ARA&A* 31, 345  
 Siegel M.H., Majewski S.R., Reid I.N., Thompson I.B., 2002, *ApJ* 578, 151  
 Smith L.F., Meynet G., Mermilliod J.-C., 1994, *A&A* 287, 835  
 Street R.A., Pollacco D.L., Fitzsimmons A., Keenan F.P., Horne K., Kane S., Collier Cameron A., Lister T.A., Haswell C.A., Norton A.J., Jones B.W., Skillen I., Hodgkin S., Wheatley P., West R., Brett D., 2003, *ASP Conf. Ser. 294: Scientific Frontiers in Research on Extrasolar Planets*, 405  
 Weidemann V., 1990, *ARA&A* 28, 103  
 Willems B., Kolb U., 2002, *MNRAS* 337, 1004  
 Willems B., Kolb U., 2003, *MNRAS* 343, 949  
 Willems B., Kolb U., 2004, *A&A* 419, 1057

This paper has been typeset from a  $\text{\TeX}/\text{\LaTeX}$  file prepared by the author.